IJE TRANSACTIONS B: Applications Vol. 25, No. 4, (November 2012) 315-324

International Journal of Engineering

Journal Homepage: www.ije.ir

Extracting Vessel Centerlines From Retinal Images Using Topographical Properties and Directional Filters

R. Kharghanian*, A. R. Ahmadyfard

Department of Electrical and Robotic Engineering, shahrood university of technology, Shahrood, Iran

PAPER INFO

Paper history:
Received 3 January 2012
Received in revised form 27 April 2012
Accepted 30 Agust 2012

Keywords:
Retinal Image
Blood Vessel Segmentation
Topographic Properties
Grouping

ABSTRACT

In this paper, we consider the problem of blood vessel segmentation in retinal images. After enhancing the retinal image we use green channel of images for segmentation as it provides better discrimination between vessels and background. We consider the negative of retinal green channel image as a topographical surface and extract ridge points on this surface. The points with this property are located on the centerline of vessels. In presence of noise and non-uniform illumination, the extracted ridge points appear as separated points which consist parts of vessel centerline. In order to connect separated ridge points and extending them for thin vessel extraction, we introduce a bank of directional filters to determine proper direction for extending the ridge end points. The ridge end points grow to provide link between separated parts of centerline using the introduced procedure. The result of experiment on images in the DRIVE database shows the proposed method outperforms the existing methods. Performance of the proposed method was evaluated based on accuracy, false positive and false negative criteria.

doi: *10.5829/idosi.ije.2012.25.04b.07*

1. INTRODUCTION

Automated blood vessel segmentation in retinal images is an applicable task for diagnosing many eye diseases. This can help a specialist for fast and accurate analysis of vessels from eye image. There are several reasons which make the automatic vessel detection in retinal images difficult. First, a considerable part of vessel network in retinal image is constructed from thin vessels with no significant difference between their intensity of vessels and background parts of the image. In the presence of imaging noise the segmentation of thin vessel is even more difficult. Second, as the background of retinal image has a non-uniform illumination, the modeling of image background is a challenge. This problem becomes more serious at optic disk and fovea regions (see Figure 1). The reported methods in the literature for the addressed problem can be divided into two main categories. The methods based on classifying the image pixels in feature space are placed in the first category. In [1], a method for extracting features from retinal images using Gabor filter was proposed. Using four features from the filter bank and the intensity of green channel a feature vector with five features is extracted. The probability density function of pixels on the vessels and non-vessels in feature space is estimated using a Gaussian Mixture Model in the training phase. In the test stage, each pixel of the retinal image is classified into one of two categories: vessel and non - vessel. The classification is performed by a Bayesian classifier based on the estimated density functions for the two classes [19]. The authors in [2] used two features extracted from perpendicular line operators to characterize a pixel on the vessel. The green channel intensity of the retinal image besides these two features pixels on the vessels and background are described. Using a set of vessel and non-vessel pixels in training stage a Support Vector Machine (SVM) classifier is set. In the same manner for each pixel of retinal test image the feature vector is constructed and used for classification. The methods in the second category attempt to model vessels in fundus images. Using image processing tools, the retinal image is analyzed to find regions which properly match the model of vessel.

In this paper, we present an algorithm for retinal blood vessel segmentation using topographic model of vessels. Our method has the following three main phases: 1) image enhancement to increase the contrast of retinal image specially for thin vessels and also in

*Corresponding Author Email: r_kharghanian@yahoo.com (R. Kharghanian)

optic disk and fovea regions; 2) extraction of vessels centerline; 3) construction of vessels using multiscale morphological filtering and region growing approach.

The main problem in previous segmentation methods is capability of detection of thin vessels and vessels in low contrast regions. As stated by other researchers except for [3], preprocessing has an important role in vessel segmentation. We propose to enhance retinal image using following three steps. In the first step a Power Law transformation, known as Gamma transformation, is used to stretch low intensity levels [17]. Then, we use Gabor filter bank to highlight patterns with vascular structure. At the end, a nonlinear transformation is used to intensify thin vessel values respect to its neighbors' values. This process is based on modification of the extracted Wavelet coefficients from retinal image [7].

Considering 2D retinal image as a topographic surface, ridges are natural indicators of vessels. By linking detected ridge points, the centerline of vessels where the image intensity is maxima can be detected. Points on the extracted centerlines are used as seed points for an iterative region growing process. On each step, the algorithm uses one level of the multiscale representation of the vascular structure based on morphological approach with variable sized structuring elements in order to reconstruction of vessel's width. Figure 2 illustrates a block diagram of our proposed scheme.

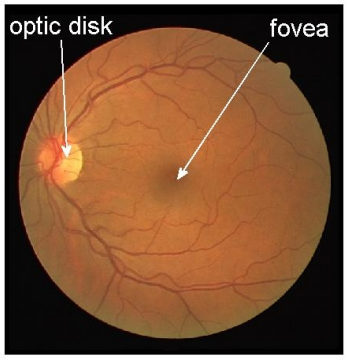

Figure 1. Disk and Fovea regions

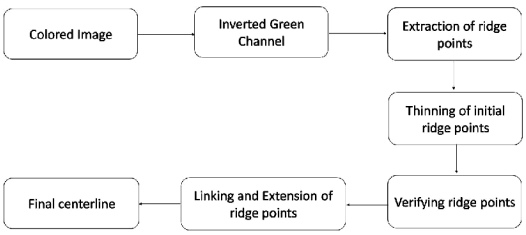

Figure 2. Block diagram of the proposed vessels segmentation method.

The rest of the paper organized as follows. In section II, the proposed method is described. In Section III, the experimental results are presented and the performance of proposed method is compared to a number of recent methods. We finally draw the paper to conclusion in Section IV.

2. PROPOSED METHOD

2. 1. Selection of the Monochromatic Image Representation In [3], the use of different color systems for segmenting vessels in retinal images has been reported. The green component of the original RGB image, the luminance channel of NTSC color space, and the a^* component of the $L^*a^*b^*$ system [11] are compared. In this comparison [3], it has been stated that the green component shows a higher vessel/background contrast than the luminance channel for both DRIVE [13] and STARE [14] databases. The vessels in the component derived from the $L^*a^*b^*$ representation clearly stand out from the background in STARE but for DRIVE did not present enough quality for a vascular segmentation task. Based on this result in this work the inverted green channel is selected for vessel segmentation process. The inversion of the green channel results observing vessels brighter than background.

2. 2. Image Preprocessing Preprocessing is an important step in vessel segmentation, mainly of the closeness of the intensity of image for thin vessels and background. Our endeavor is to achieve a significant distinction between vessels and non-vessels using several stages.

In order to enhance the contrast of vessel/background in the thin blood vessel, first a gamma correction is applied on the inverted green channel of the retinal image [17], [4]. Considering the inverted green channel of the retinal image as fG correction for pixel (i, j) is performed as follows:

$$fC_{ij} = \left[\frac{fG_{ij} - fG_{MIN}}{fG_{MAX} - fG_{MIN}} \right]^r \quad (1)$$

where, fG_{MIN} and fG_{MAX} are minimum and maximum intensity of image, fG and r is correction parameter. The intensified image is denoted by fC.

Since retinal blood vessels can appear in any direction, a directional filter has been chosen to extract vessel patterns. 2-D Gabor wavelet has directional selectiveness capability of detecting oriented features and fine tuning to specific frequencies [5, 6]. This latter property is especially important to filter out the background noise of the fundus image. The 2-D Gabor wavelet is defined as:

$$\psi_G(\vec{x}) = \exp(j\vec{k}_0\vec{x})\exp(-\frac{1}{2}|A\vec{x}|^2) \quad (2)$$

where, $A = diag\left[\varepsilon^{-1/2} \quad 1\right]$, $(\varepsilon \geq 1)$ is a 2×2 diagonal matrix that defines the anisotropy of the filter, i.e., its elongation in any desired direction. The Gabor wavelet is actually a complex exponential modulated Gaussian, where, $\vec{k}_0$ is a vector that defines the frequency of the complex exponential. The Continuous wavelet transform is defined in terms of the scalar product of fC with the transformed wavelet $\psi_{\vec{b},\theta,a}$.

$$\begin{aligned} T_\psi(\vec{b},\theta,a) &= C_\psi^{-1/2}\langle\psi_{\vec{b},\theta,a}|f\rangle \\ &= C_\psi^{-1/2}a^{-1}\int\psi^*(a^{-1}r_{-\theta}(\vec{x}-\vec{b}))f(\vec{x})d^2\vec{x} \end{aligned} \quad (3)$$

where, $C_\psi, \psi, \vec{b}, \theta$ and a denote the normalizing constant, analyzing wavelet, the displacement vector, the rotation angle, and the dilation parameter (also known as scale), respectively. ψ^* denotes the complex conjugate of ψ. The wavelet transform can be easily implemented using the fast Fourier transform algorithm and the equivalent Fourier definition of the wavelet transform [5].

$$\begin{aligned} T_\psi(\mathrm{b},\theta,a) &= C_\psi^{-1/2}\langle\psi_{\vec{\mathrm{b}},\theta,a}|f\rangle \\ &= C_\psi^{-1/2}a\int\exp(i\vec{b}\vec{k})\hat{\psi}^*(ar_{-\theta}(\vec{k}))\hat{f}(\vec{k})d^2(\vec{k}) \end{aligned} \quad (4)$$

where, the hat denotes a Fourier transform.

The maximum modulus of the wavelet transform over all angles, from 0° up to 179° at step of 10°, for one scale is taken. The enhanced image I_G is determined based on the direction θ which provides the maximum Gabor response.

$$I_G = \max_\theta |T_\psi(\vec{b},\theta,a)| \quad (5)$$

As the contrast at retinal border is very strong, the response of gabor wavelet produce a false edge.

To reduce this effect before applying wavelet transform, we pad the background pixels at the neighborhood of retinal border with a gray value equal to average of neighboring retinal pixels. For this task, we have used an iterative algorithm as proposed in [1]. This algorithm would help to remove the strong contrast between the retinal fundus and the region outside the aperture. Hence, the output of the wavelet transform doesn't provide strong edge at retinal borders.

As the contrast of thin vessels from the background is low, segmentation of thin vessels even after wavelet analysis is imperfect. We used the method [7] to modify wavelet coefficients in such a way that improve the contrast. Equation (6) shows the relation between wavelet coefficients before and after this transformation. x is the intensity value of pixel in I_G image and $y_c(x)$ is its value after transformation. p is a parameter which determines the degree of nonlinearity ($0 < p < 1$) and s introduces dynamic range compression.

$$y_c(x) = \begin{cases} 1 & x < c\sigma \\ \frac{x-c\sigma}{c\sigma}\left(\frac{m}{c\sigma}\right)^p + \frac{2c\sigma - x}{c\sigma} & c\sigma \leq x < 2c\sigma \\ \left(\frac{m}{x}\right)^p & 2c\sigma \leq x < m \\ \left(\frac{m}{x}\right)^s & x \geq m \end{cases} \quad (6)$$

Using a nonzero s enhances the faintest edges and softens the strongest edges at the same time. c is a normalization parameter and σ is the standard deviation of the background noise. The m is the intensity value under which output intensity values are amplified. This value depends obviously on the pixel values inside the image. A proper value for m can be derived from percentage of maximum Gabor output, and standard noise deviation: $m = k_c M - c\sigma$. Figure 3 shows the colored image, the inverted of green channel, gamma corrected and padded image.

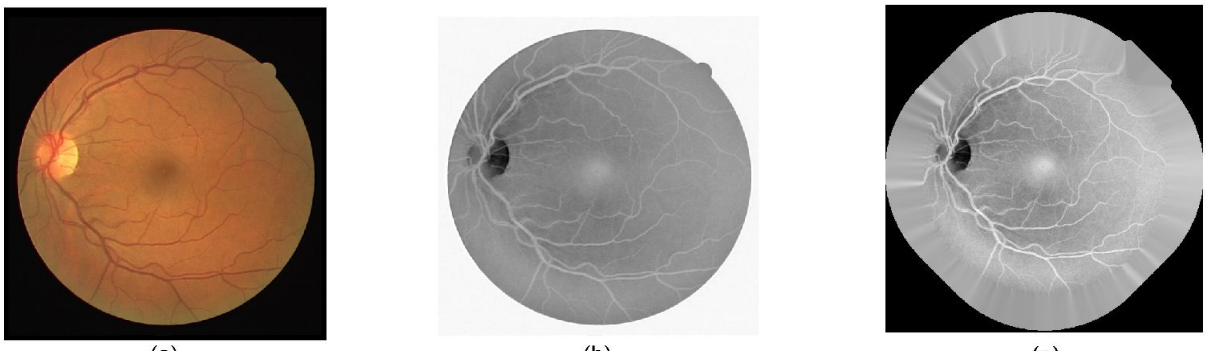

(a) (b) (c)

Figure 3. a) Colored image b) inverted of green channel c) gamma corrected and padded image.

2. 3. Topographic Features and Ridge Detection Considering a 2D image as a topographic surface, each pixel of image based on geometrical property of surface at the pixel takes one of twelve topographic labels: peak, peat, saddle, ridge, ravine, ridge saddle, ravine saddle, slop upward, slop downward, convex saddle hill, concave saddle hill and flat [8].

The image pixels on retinal vessels have ridge topographic property. Ridges are invariant to affine transformations and can be detected in different image modalities. Roughly speaking, ridges are defined as points where the image has an extremum in the direction of the largest surface curvature. Strictly speaking, a ridge occurs where there is a local maximum in one direction. By connecting ridge points a ridge line is obtained which indicates the centerline of vessels. For a continuous surface defined by the equation $z = f(x, y)$ let ∇f be the gradient vector of the function and $\|\nabla f\|$ be the gradient magnitude. Hessian matrix can be defined as:

Hessian matrix can be defined as:

$$H = \begin{bmatrix} \frac{\partial^2 f(x,y)}{\partial x^2} & \frac{\partial^2 f(x,y)}{\partial xy} \\ \frac{\partial^2 f(x,y)}{\partial xy} & \frac{\partial^2 f(x,y)}{\partial y^2} \end{bmatrix} \quad (7)$$

where, u_1 and u_2 are the unit eigenvectors of H and λ_1, λ_2 are corresponding eigenvalues. A point is called a ridge if and only if it satisfies one of the following three sets of conditions.

$$\|\nabla f\| \neq 0, \lambda_1 < 0, \nabla f . u_1 = 0 \quad (8)$$

$$\|\nabla f\| \neq 0, \lambda_2 < 0, \nabla f . u_2 = 0 \quad (9)$$

$$\|\nabla f\| = 0, \lambda_1 < 0, \lambda_2 = 0 \quad (10)$$

In order to extract ridge points in a digital image, the first and second partial derivative need to be estimated. We use the discrete Chebyshev polynomials up to the third degree (N=3) to estimate derivatives of a digital image. The $(p,q)th$ partial derivative at (x, y), (p along the x axis and q along the y axis) is approximated as:

$$f^{(p,q)}(x, y) = \sum_{i=-N}^{N} \sum_{j=-N}^{N} f(x, y) h(i, p) h(j, q) \quad (11)$$

where, $f(x,y)$ is the grayscale image, and $h(i, p)$ and $h(j,q)$ are unweighted smoothing differentiation filters based on discrete Chebyshev polynomials [9]:

$$h(i,0) = -\frac{3\left[5i^2 - \left(3N^2 + 3N - 1\right)\right]}{(2N-1)(2N+1)(2N+3)} \quad (12)$$

$$h(i,1) = \frac{5\left[7(3N^2 + 3N - 1)i^3 - 5(3N^4 + 6N^3 - 3N = 1)i\right]}{(N-1)N(N+1)(N+2)(2N\_1)(2N+1)(2N+3)} \quad (13)$$

$$h(i,2) = \frac{30\left[3i^2 - N(N+1)\right]}{N(N+1)(2N-1)(2N+1)(2N+3)} \quad (14)$$

By this definition, hessian matrix can be written in form of:

$$H = \begin{bmatrix} f^{(2,0)}(x,y) & f^{(1,1)}(x,y) \\ f^{(1,1)}(x,y) & f^{(0,2)}(x,y) \end{bmatrix} \quad (15)$$

Usually, an interesting topographic label will not occur precisely at the center of pixel. If we assign to pixel label which is belong to the pixel's center point, a misclassification would occur. We used Wang et al. [8] method to solve this problem. The eigenvectors u_1 and u_2 at the center of each pixel are estimated using two orthogonal vectors which are closest to two of the four natural directions orientations 0°, 45°, -45° and 90°.

The explained ridge extraction method yields ridge points which are good candidates for centerline of retinal vessels.

2. 4. Noise Reduction By applying the ridge extraction algorithm to the enhanced input image I_G, a binary image with points on vessel centerlines is produced. As the width for extracted vessel centerlines is more than one pixel, we use morphological thinning to obtain an image on which vessel centerlines have one pixel width. The result image is denoted by I_R. I_R contains considerable false positives, that is, the pixels which belong to the background but labeled as ridge centerlines. We need to filter out the false ridge points as much as possible.

We have developed an algorithm to achieve this aim. The proposed method has two major steps. First determining eight-adjacency connected components of the extracted ridge image, I_R. The components with more than a predefined number of pixels (l) are confirmed as vessel centerlines. Let us denote the image of remaining components by I_{RS}. The components in this image need to be rechecked for filtering out false ridge points. We first determine four-adjacency connected components of I_{RS}. For each component of the resulting image, the validation process is performed as follows:

a. Determine position of the middle pixel.
b. Consider an $L \times L$ window centered at the middle pixel on the negative green channel of retina, I_{Gm}.
c. Convert the extracted window into a binary image using a threshold equal to geometric mean between the average and maximum values pixels in the window.

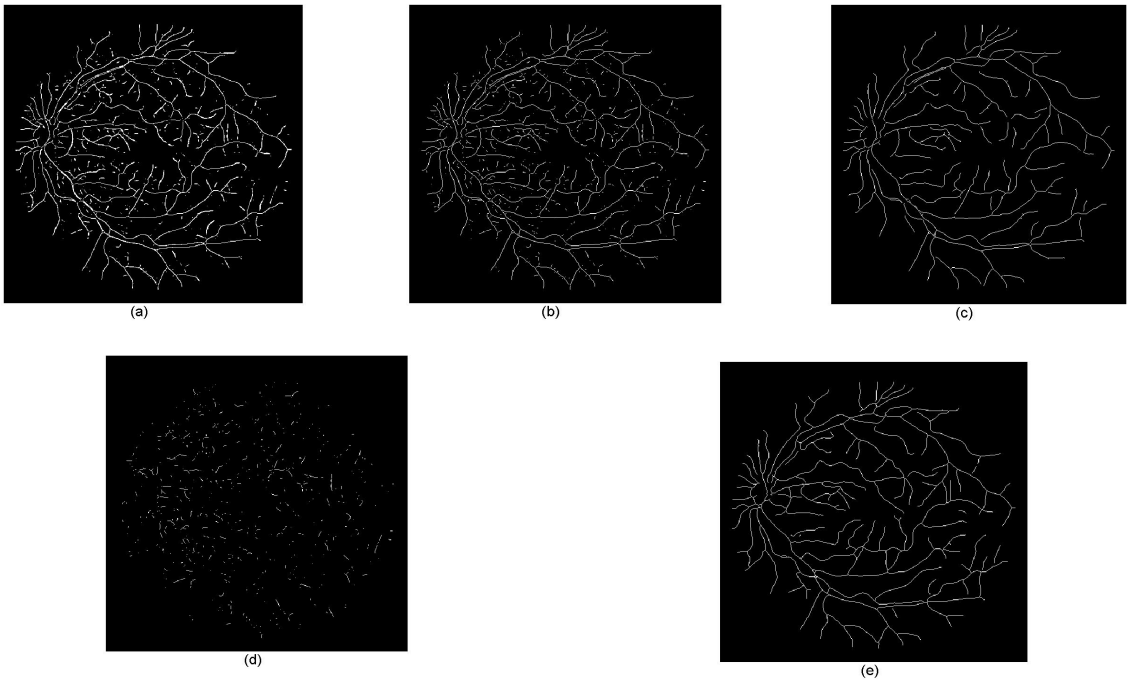

Figure 4. a) initial ridge points, b) thinned ridges, c) long strings, d) ridge points need to be validated, e) final ridge points

d. Perform an AND operation between the binary window and the corresponding window from the ridge points.
e. Remove the under consideration component if the number of pixels with value one in the result window is less than half of number of pixels for the component.

The final denoised image I_{Rd} formed by long ridge strigns and verified ridge points/lines. Figure 4 illustrates results in applying mentioned algorithm. Comparing Figures 4-c and 4-e, during the proposed process, same points on thin vessels are confirmed as ridge points. They will be completed in the next stages.

2. 5. Linking and Extending the Ridge Points The extracted ridge points are a set of strings which needs to be completed for two reasons. First broken strings which are parts of a centerline need to be linked together using a grouping process. Second the extracted centerlines need to be extended to detect thin vessels.

We propose a grouping algorithm which starts with finding end-points of extracted strings. End-points are used as the starting points for this algorithm. This process is an iterative algorithm which detects endpoints using the morphological Hit-or-Miss transform [17] as follows:

$$End - pts = \bigcup_{k=1}^{8} \left(f_R \otimes B^k \right) \quad (16)$$

where, the B^k are the structure elements used in this process shown in Figure 5.

At each extracted end point, we investigate if there is a chance for extension of the end point. For this purpose, a set of directional masks so called Directional Mask Bank (DMB) is designed. The DMB is made up of eight masks with size 15×15 pixels, as shown in Figure 6.

The most probable region which ridges can be extended is determined using these masks.

Each filter of DMB is placed on the binary formed with the detected ridges at an end-point location, the result of an AND operation between the filter and the ridge point image is a number of pixels. with the ridge point image. That filter determines roughly the direction for extension of the end-point.

Figure 7 demonstrates the responses over eight masks.

In order to refine direction for extending each end points another filtering procedure is proposed. Consider a filter bank where each filter is a L pixel line in a $(2L-1)\times(2L-1)$ window. Each filter line (L pixels) starts from the center of window and ends at a pixel on circumference of the window. Figure 8 shows two filter lines with $L=8$ in 15×15 window at 0 and 45 degree

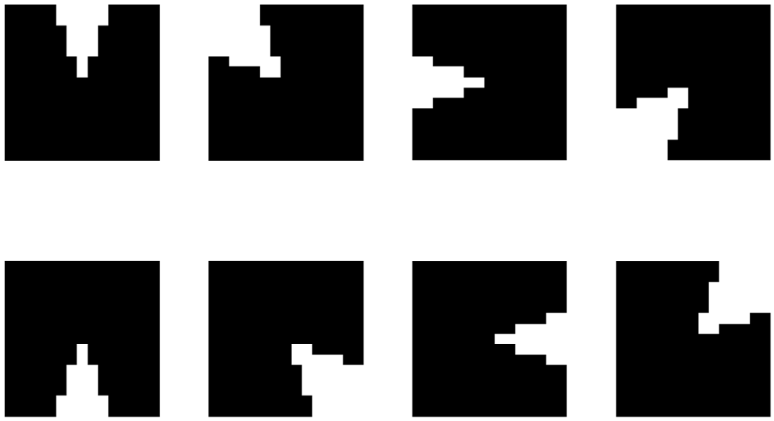

Figure 5. Directional Mask Bank (DMB), eight masks with size 15×15 pixels in different orientation

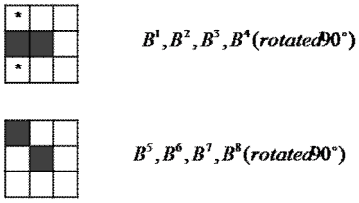

Figure 6. The end-point detectors[17]

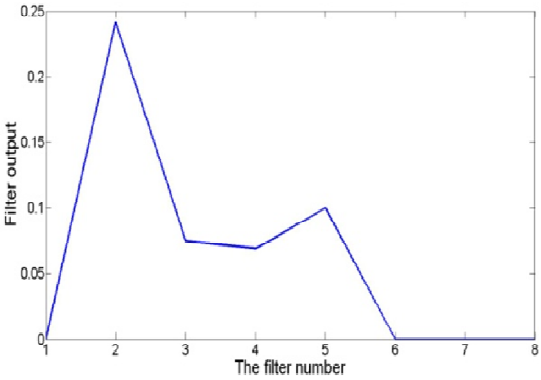

Figure 7. DMB response

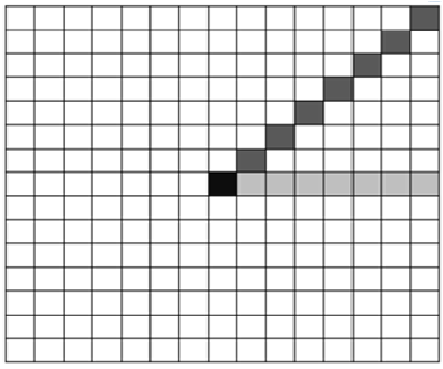

Figure 8. Two line filters in a 15×15 window.

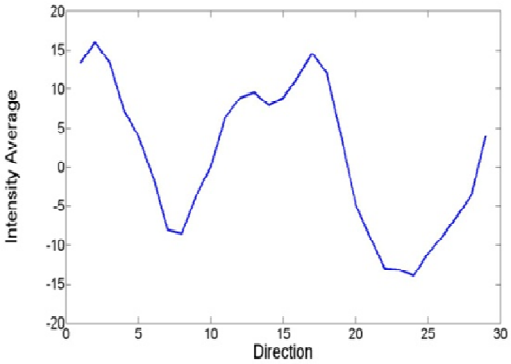

Figure 9. Average value of lines in extension region

One of the eight filters provides the maximum number of pixels as the result of AND operation. After determining rough direction of possible extension of ridge points in the previous stage, only few number of line filters falls within the determined sector. Along each line filter, the average intensity of pixels from the original retinal image (negative green channel) is evaluated. The line filter with largest average is selected as the most probable direction which vessel can be extended. Figure 9 shows the average intensity along line filters at the end point.

Figure 10 shows a selected window of ridge image 4-e and the intermediate and final process of linking stage.The statistics for average of intensity along line filters can be used as to accept extension of ridge string along the candidate direction or refuse to continue. Let consider σ and μ as the standard deviation and the mean for the average intensity of line filters at an end point. We use the ratio σ/μ as a criterion to accept extension of a ridge string under consideration end point. If this ration is more than a predefined value, it shows that along the candidate line filter there is a vessel.

Figure 10. a) Ridge point, b) Vessel centerlines

Figure 11. (a) A selected window of ridge image for extension and (b, c) Intermediate process (d) After complete linkage.

TABLE 1. Values of the parameters used for retinal image enhancement

Parameter	r	m	c	σ	p	k_c
Value	1.5	3	3	6	0.8	0.3

In contrast, low value for σ/μ means we have a noisy region and extension of end point must be quitted. If the extension of ridge string is confirmed, we extend the current end point along the candidate line filter and the new end point is defined the end of line filter. This process is iteratively run until all image end points terminated.

Figure 11 shows initial ridge points and the extended vessel centerlines for a retinal image.

3. EXPERIMENTAL RESULTS

We tested our method on retinal images in the DRIVE database. The database is publicly available with manual segmentation [13]. The DRIVE database consists of 40 images where seven of which present pathology, along with manual segmentations of the vessels. The images are captured in digital form from a Canon CR5 nonmydriatic 3CCD camera at 45° field of view (FOV). The images are of size 768×584 pixels, eight bits per color channel and have a FOV of approximately 540 pixels in diameter. The images are in compressed JPEG format, which is unfortunate for image processing but is commonly used in screening practice. The 40 images have been divided into training and test set, each set containing 20 images. For each image in the training set, there are three images with pathology. They have been manually segmented by ophthalmologists. The images in the training set were segmented once, while images in the test set were segmented twice, resulting in sets A and B. The observers of sets A and B produced similar segmentations. In set A, 12.7% of pixels where marked as vessel, against 12.3% vessel for set B. We implemented the proposed method using the following settings. In Gabor filter bank we set ε parameter to 2 and $\bar{k}_0 = [0.5 \quad 2.5]$. This setting empirically has been selected to yield the best discrimination between the blood vessels from background. We have imperially chosen proper values for the enhancement method as reported in Table 1.

The vessel segmentation using the proposed method was performed on the DRIVE database. The segmentation result of the method was compared against the human observer reference provided in the database.

Accordingly, the performance of the proposed method is evaluated using accuracy, sensitivity and specificity criterions. The accuracy is defined as the ratio of the total number of correctly classified pixels by the total number of pixels in the image. Other important measures are sensitivity and specificity. The true positive fraction (TPF), also called "sensitivity", is determined by dividing the number of pixels correctly classified as vessel pixels (TP) by the total number of vessel pixels:

$$TPF = \frac{TP}{P} = \frac{TP}{TP + FN} = sensitivit\ y \tag{17}$$

TABLE 2. Performance of vessel segmentation methods (DRIVE database)

Segmentation Method	Average accuracy (standard deviation)	True Positive Fraction (sensitivity)	False Positive Fraction ($1-specificity$)
Proposed	**0.9464(0.0063)**	**0.7690**	**0.0259**
Staal et al.[18]	0.9442(0.0065)	0.7194	0.0227
Niemeijer [15]	0.9417(0.0065)	0.6898	0.0304
Soares et al. [1]	0.9460(0.0060)	0.7344	0.0226
Mendonça et al. [3]	0.9452(0.0062)	0.7344	0.0236
Ricci et al. [2]	0.9428(0.0073)	0.6957	0.0198
2nd Human observer [13]	0.9473(0.0048)	0.7761	0.0275

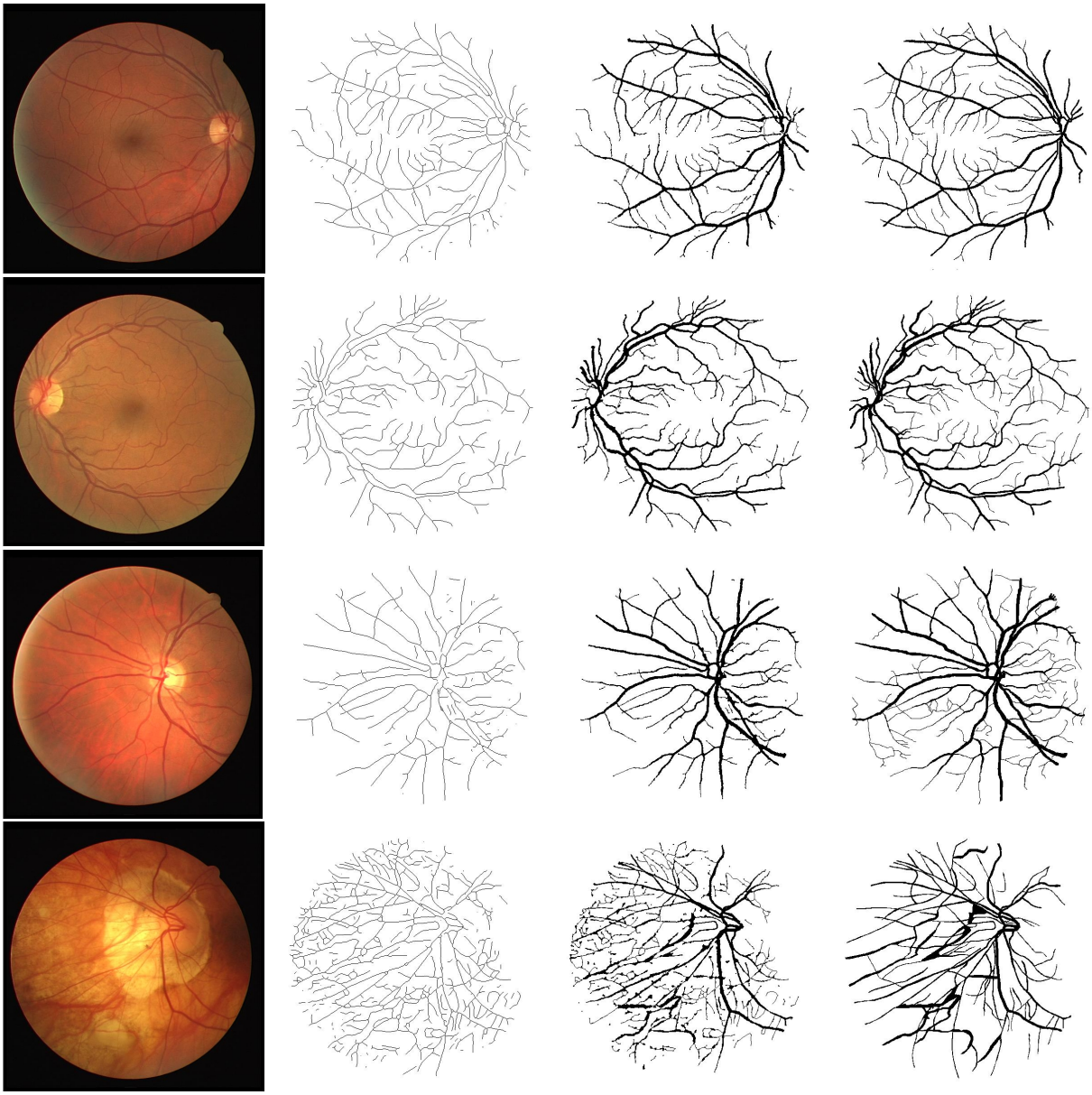

Figure 12. The left column: two samples of retinal images of DRIVE database. The next column: the extracted centerline. The third column from the left: the final result after region growing. The last column: the expert groundtruth.

where, FN is the number of pixels incorrectly classified as non-vessel pixels. The false positive fraction (FPF) is the number of pixels incorrectly classified as vessel pixels (FP) divided by the total number of non-vessel pixels:

$$FPF = \frac{FP}{N} = \frac{FP}{FP + TN} = 1 - specificit\ y \quad (18)$$

Here, TN is the number of pixels correctly classified as non-vessel pixels. The axes of the plot are rescaled so the true positives and false positives vary between 0 and 1.

The accuracy (ACC) for one image is the fraction of pixels correctly classified:

$$ACC = \frac{FP + TP}{N + P} = \frac{TP + TN}{TP + FN + FP + TN} \quad (19)$$

The maximum average accuracy (MAA) will be the average value of the accuracy for all images.

Table 2 presents the result of experiment on DRIVE database. This table shows the maximum average accuracy, standard deviation, True Positive Fraction and False Positive Fraction calculated with our method. We compare the performance of our algorithm to that of Mendonça et al. [3], Staal et al.[18] and Niemeijer[15] using their publicly available results. To compare our method with the methods of Soares et al. [1] and Ricci et al. [2], we implemented those methods except that for Soares et al. [1]. we used 700,000 instead of one million pixel samples.

The first row of the table is the result for the proposed method which is compared against other methods and manually segmentation of the human observer. As the table shows from the accuracy point of view the proposed method outperforms other methods. However, the performance of the method is slightly below the manually segmentation provided by the human observer. In contrast to two earlier criterions, the false positive for a segmentation method is desired to be as small as possible. From the false positive point of view, the proposed method outperforms the method of Niemeijer [5] but it is slightly below the other methods.

In Figure 12, the final result of vessel segmentation on two retinal images from DRIVE database have been shown.

The retinal images have been shown on the first column from the left. The second and third columns show the result of vessel centerline extraction (the proposed method) and the result of thickening on the extracted centerlines respectively. First column from the right shows the manual segmentation provided by an expert.

4. CONCLUSION

The problem of extracting vessel centerline from retinal image was addressed. In presence of noise and imperfect illumination condition, we enhance the negative green channel of retinal image as input for the proposed system. Using topographical features, we extract ridge points as candidate for vessel centerlines. The separate extracted points were linked to construct vessel using introduced directional filters. This filters measure possibility for presence of a vessel in each direction at an end point on each extracted ridge string. Based on this procedure ridge strings are linked together and extended to extract thin vessels. The result of experiments showed the proposed method provides better accuracy in compare with other methods.

5. REFERENCES

1. Soares, J.V.B., Leandro, J.J.G., Cesar, R.M., Jelinek, H.F. and Cree, M.J., "Retinal vessel segmentation using the 2D Gabor wavelet and supervise classification", ***IEEE Transactions on Medical Imaging***, Vol. 25, No. 9, (2006), 1214–1222.
2. Ricci E. and Perfetti, R., "Retinal blood vessel segmentation using line operators and support vector classification", ***IEEE Transactions on Medical Imaging***, Vol. 26, No. 10, (2007).
3. Mendonça, A. M. and Campilho, A., "Segmentation of Retinal Blood Vessels by Combining the Detection of Centerlines and Morphological Reconstruction", ***IEEE Transactions On Medical Imaging***, Vol. 25, No. 9, (2006).
4. Chang, C.-C., Lin, C.-Ch., Pai, P.-Y. and Chen. Y.-Ch., "A Novel Retinal Blood Vessel Segmentation Method Based on Line Operator and Edge Detector", ***Fifth International Conference on Intelligent Information Hiding and Multimedia Signal Processing***, (2009).
5. Antoine, J.-P., Carette, P., Murenzi, R. and Piette, B., "Image analysis with two-dimensional continuous wavelet transform", ***Signal Process***, Vol. 31, (1993), 241–272.
6. Arnéodo, A., Decoster, N. and Roux, S. G., "A wavelet-based method for multifractal image analysis. I. Methodology and test applicationsnon isotropic and anisotropic random rough surfaces", ***European. Physical Journal- Applied physics***, Vol. 15, (2000), 567–600.
7. Starck, J.L., Murtagh, F., Candès, E. J. and Donoho, D. L., "Gray and Color Image Contrast Enhancement by the Curvelet Transform", ***IEEE Transactions On Image Processing***, Vol. 12, No. 6, (2003).
8. Wang L. and Pavlidis, T., "Direct Gray-Scale Extraction of Features for Character Recognition", ***IEEE Transactions On Pa'itern Analysis And Machine Intelligence***, Vol. 15, NO. 10, (1993).
9. Meer, P. and Weiss, I., "Smoothed differentiation filters for images", Center for Automatic Research University of Maryland, (1989).
10. Zwiggelaar, R., Astley, S.M., Boggis, C. R. M. and Taylor, C. J., "Linear structures in mammographic images: Detection and classification", ***IEEE Transactions On Medical Imaging***, Vol. 23, No. 9, (2004), 1077–1086.
11. Pratt, W.K., "Digital Image Processing", 3rd ed. New York, Wiley, (2001).
12. Theodoridis, S. and Koutroumbas, K., "Pattern Recognition", 1st ed., Burlington, MA, Academic, (1999).
13. Niemeijer, M. and van Ginneken, B., (2002), [Online] Available: Available:http://www.isi.uu.nl/Reseach/Databases/DRIVE/results.php
14. Hoover, A., STARE database [Online] Available: Available: http://www.ces.clemson.edu/~ahoover/stare

15. Niemeijer, M., Staal, J., van Ginneken, B., Loog, M. and Abràmoff, M.D., "Comparative study of retinal vessel segmentation methods on a new publicly available database", ***in Proceeding of SPIE Medical Imaging, M. Fitzpatrick and M. Sonka, Eds.,*** Vol. 5370, (2004), 648–656.
16. Hoover, A., Kouznetsova, V. and Goldbaum, M., "Locating blood vessels in retinal images by piecewise threshold probing of a matched filter response", ***IEEE Transactions On Medical Imaging***, Vol. 19, No. 3, (2000), 203–211.
17. Gonzalez, R.C. and Woods, R.E., Digital Image Processing, 3rd ed., Prentice hall, (2008).
18. Staal, J., Abramoff, M. D., Niemeijer, M., Viergever, M. A. and Ginneken, B.V., "Ridge-based vessel segmentation in color images of the retina", ***IEEE Transactions On Medical Imaging***, Vol. 23, No. 4, (2004), 501–509.
19. Duda, R. O., Hart, P. E. and Stork, D. G., "Pattern Classification", 2nd ed., New York, Wiley, (2001).

Extracting Vessel Centerlines From Retinal Images Using Topographical Properties and Directional Filters

R. Kharghanian, A. R. Ahmadyfard

Department of Electrical and Robotic Engineering, shahrood university of technology, Shahrood, Iran

P A P E R I N F O

Paper history:
Received 3 January 2012
Received in revised form 27 April 2012
Accepted 30 Agust 2012

Keywords:
Retinal Image
Blood Vessel Segmentation
Topographic Properties
Grouping

چکیده

در این مقاله مسئله استخراج رگ‌های شبکیه چشم را از تصویر شبکیه مورد مطالعه قرار داده‌ایم. از آنجایی که کانال سبز تصویر بهترین کنتراست بین رگ و غیر رگ را داراست، از این کانال برای جداسازی رگ‌ها استفاده کرده‌ایم. پس از ارتقاء تصویر معکوس کانال سبز، آن را به صورت یک رویه توپوگرافیکی در نظر گرفته و نقاط ناودانی بیرون را از آن استخراج می‌کنیم. این نقاط بر روی مرکز رگ‌ها قرار دارند. در حضور نویز پیش‌زمینه و توزیع غیریکنواخت روشنایی در تصویر برداری، مراکز رگ‌ها به درستی استخراج نمی‌شوند. نقاط استخراج شده جدا از یکدیگر می‌باشند و تنها بخشی از خط مرکزی رگ را تشکیل می‌دهند. برای اتصال نقاط مجزا و گسترش آن‌ها با هدف استخراج رگ‌های باریک روش جدیدی پیشنهاد شده است. در این روش بانکی از فیلترهای جهت‌دار طراحی نموده‌ایم که جهت مناسب برای رشد خط مرکزی رگ را تخمین می‌زند. به کمک این روش نقاط انتهایی رشته خطوط ناودانی رشد داده می‌شوند تا خطوط مرکزی رگ‌ها به صورت رشته‌های پیوسته گسترش یابند. نتایج حاصل از آزمایشات بر روی پایگاه داده DRIVE نشان دهنده برتری روش پیشنهاد شده نسبت به روش‌های موجود است. این برتری با معیار صحت، میزان عدم اشتراک و حساسیت سنجیده شده‌است.

doi: *10.5829/idosi.ije.2012.25.04b.07*